Editors' Suggestion

Quantum Mpemba Effect in a Quantum Dot with Reservoirs

Amit Kumar Chatterjee,[1,*] Satoshi Takada,[2,†] and Hisao Hayakawa[1,‡]
[1]Yukawa Institute for Theoretical Physics, Kyoto University, Kitashirakawa Oiwakecho, Sakyo-ku, Kyoto 606-8502, Japan
[2]Department of Mechanical Systems Engineering and Institute of Engineering, Tokyo University of Agriculture and Technology, 2-24-16 Naka-cho, Koganei, Tokyo 184-8588, Japan

(Received 14 April 2023; accepted 17 July 2023; published 22 August 2023)

We demonstrate the quantum Mpemba effect in a quantum dot coupled to two reservoirs, described by the Anderson model. We show that the system temperatures starting from two different initial values (hot and cold) cross each other at finite time (and thereby reverse their identities; i.e., hot becomes cold and vice versa) to generate *thermal* quantum Mpemba effect. The slowest relaxation mode believed to play the dominating role in Mpemba effect in Markovian systems does not contribute to such anomalous relaxation in the present model. In this connection, our analytical result provides necessary condition for producing quantum Mpemba effect in the density matrix elements of the quantum dot, as a combined effect of the remaining relaxation modes.

DOI: 10.1103/PhysRevLett.131.080402

Introduction.—The Mpemba effect (MPE) is a fascinating counterintuitive phenomenon indicating hot liquid can freeze faster than cold liquid, observed long ago by Aristotle [1] and rediscovered by Mpemba and Osborne [2]. Various mechanisms have been proposed to explain MPE [3–12], still lacking any unified theory. In fact, several experiments have raised questions regarding the validity of MPE [13]. A problem regarding the correct definition of MPE for various systems [2,14–16] is the complexity of the phase transitions associated with these cases. In this connection, the experimental observation of MPE in a colloidal system without phase transition is remarkable [17].

Although MPE was originally perceived as a thermal phenomenon of anomalous cooling in liquids, later it was identified as a more general anomalous relaxation occurring in a wide variety of systems, including colloids [17,18], granular gases [19–24], optical resonators [25–27], inertial suspensions [28,29], Markovian models [30–33], and others [34–41]. To analyze MPE in classical systems, time variations of temperature [22,28], energy [21], and viscocity [28] have been employed in granular gases and inertial suspensions whereas entropic distance-from-equilibrium functions have been applied to Markov jump processes [30,31] and colloidal systems [17]. Recently, nontrivial connections between thermal and entropic MPEs have been exploited [42] and the crucial dependence of MPE on the choice of the observables has been studied [43].

In spite of substantial works on the classical MPE, investigations on quantum Mpemba effect (QMPE) have been few [44–48]. The studies of QMPE have been based on the entropic distance-from-equilibrium functions [45,46,48], entanglement asymmetry [47], and magnetization [44]. Importantly, QMPE lacks the analysis of temperature, and therefore the notion of thermal QMPE is missing. Secondly, the criterion for QMPE [45,48] and MPE [30,31,40] in both quantum and classical Markovian systems solely focus on the slowest relaxation mode. Complete absence of the slowest relaxation mode for certain parameter choices or initial conditions leads to exponentially faster relaxation, called *strong* MPE [17,31,49] and *strong* QMPE [45]. However, the roles of other relaxation modes in generating Markovian MPE and QMPE remain unexplored.

In this Letter, we address the abovementioned issues: (i) possibility of thermal QMPE and (ii) the role of relaxation modes other than the slowest one in producing QMPE in density matrix elements and temperature. For the demonstration of QMPE, we examine a quantum dot (QD) system coupled to two reservoirs, described by the Anderson model. The occurrence of QMPE is defined as the finite time crossing of temporal trajectories of any entity starting from two different initial conditions that reach the same steady state. We show that the system temperature exhibits thermal QMPE with the variation of control parameters. Moreover, the slowest relaxation mode does not contribute to the QMPE in the present model and we illustrate the combined role of the remaining eigenmodes in generating QMPE.

Model.—We consider a single-level quantum dot coupled to two reservoirs (L and R). The total system is described by the Anderson model with the Hamiltonian $\hat{H}_{\rm tot}=\hat{H}_s+\hat{H}_r+\hat{H}_{\rm int}$, where $\hat{H}_s, \hat{H}_r$ are the Hamiltonians for the QD and the two reservoirs, respectively, and $\hat{H}_{\rm int}$ denotes the system-reservoirs interaction. The explicit forms of the Hamiltonians are [50,51]

$$\hat{H}_s=\sum_{\sigma}\epsilon_0\hat{d}_\sigma^\dagger\hat{d}_\sigma+U\hat{n}_\uparrow\hat{n}_\downarrow, \qquad \hat{H}_r=\sum_{\gamma,k,\sigma}\epsilon_k\hat{a}_{\gamma,k,\sigma}^\dagger\hat{a}_{\gamma,k,\sigma},$$
$$\hat{H}_{\rm int}=\sum_{\gamma,k,\sigma}V_\gamma\hat{d}_\sigma^\dagger\hat{a}_{\gamma,k,\sigma}+\text{H.c.} \tag{1}$$

The parameters ϵ_0 and ϵ_k correspond to an electron energy in the QD and the reservoirs, respectively, and U is the electron-electron repulsion energy in the QD. The index σ denotes up spin ($\uparrow$) and down spin ($\downarrow$), γ represents L and R. The creation (annihilation) operators for the QD and the reservoirs are $\hat{d}^\dagger$ ($\hat{d}$) and $\hat{a}^\dagger$ ($\hat{a}$), respectively. Here $\hat{n}_\sigma = \hat{d}^\dagger_\sigma \hat{d}_\sigma$ is the number operator. The coupling strength between QD and L (R) is V_L (V_R). We adopt a model in the *wideband limit* for reservoirs [50–53]. We denote the linewidth $\Gamma = \pi\Omega V^2$ ($V^2 = V_L^2 + V_R^2$), where Ω is the density of states in the reservoirs. The chemical potentials of L (R) are μ_L (μ_R) and their temperatures are taken equal, $T_L = T_R = T$. We consider temperatures much higher than the Kondo temperature to ignore the Kondo effect [54–56]. We focus on the weak coupling to disregard cotunneling [57].

The tunneling between QD and the reservoirs means the QD has four possible states, namely the doubly occupied state ($\uparrow\downarrow$), singly occupied up-spin state ($\uparrow$), singly occupied down-spin state ($\downarrow$), and empty state, enumerated by $\alpha = 1, 2, 3, 4$, respectively. Correspondingly, the elements of the density matrix operator $\hat{\rho}$ for the QD are represented by ρ_α. Using wideband approximation, $\hat{\rho}$ reduces to a purely diagonal form [50–53] with four nonzero elements ρ_α. The dynamics of the QD is described by the quantum master equation,

$$\frac{d}{d\tau}\hat{\rho} = \hat{K}\,\hat{\rho}, \tag{2}$$

where $\tau := \Gamma t$ is the dimensionless time. The transition matrix $\hat{K}$ has the form [50,53]

$$\hat{K} := \begin{pmatrix} -2f_-^{(1)} & f_+^{(1)} & f_+^{(1)} & 0 \\ f_-^{(1)} & -f_-^{(0)} - f_+^{(1)} & 0 & f_+^{(0)} \\ f_-^{(1)} & 0 & -f_-^{(0)} - f_+^{(1)} & f_+^{(0)} \\ 0 & f_-^{(0)} & f_-^{(0)} & -2f_+^{(0)} \end{pmatrix}. \tag{3}$$

The factors $f_\pm^{(j)}$ ($j = 0, 1$) [Eq. (3)] are related to the physical input parameters as

$$f_+^{(j)} := f_L^{(j)}(\mu_L, U, \epsilon_0, T) + f_R^{(j)}(\mu_R, U, \epsilon_0, T), \quad j = 0, 1$$
$$f_\gamma^{(j)}(\mu_\gamma, U, \epsilon_0, T) := \frac{1}{1 + e^{(\epsilon_0 + jU - \mu_\gamma)/T}}, \quad \gamma = L, R, \tag{4}$$

with $f_{L,R}^{(j)}$ ($j = 0, 1$) being the Fermi-Dirac distribution. Among the parameters $f_\pm^{(j)}$ ($j = 0, 1$) in Eq. (3), only two are independent (we consider $f_+^{(j)}$ with $j = 0, 1$) because $f_-^{(j)} = 2 - f_+^{(j)}$. The exact analysis of QMPE in the QD can be performed in terms of $f_+^{(0)}$ and $f_+^{(1)}$ and Eq. (4) is used to express the results in terms of chemical potential, temperature, and the Hamiltonian parameters.

Protocol.—We use two different sets I and II of initial conditions, $\hat{\rho}^{\mathrm{I}}(\tau = 0)$ and $\hat{\rho}^{\mathrm{II}}(\tau = 0)$. Both these initial conditions are chosen in the form of the steady state distribution corresponding to the largest (zero) eigenvalue of $\hat{K}$ [Eq. (3)]. They may differ in the values of one or more input parameters. For initial condition I, we choose $\mu_L^{\mathrm{I}} \neq \mu_R^{\mathrm{I}}$, whereas for II, we take $\mu_L^{\mathrm{II}} = \mu_R^{\mathrm{II}} = \mu^{\mathrm{II}}$. For both initial conditions, the reservoirs are maintained at the same initial temperature T_i. At $\tau = 0$, we perform *instantaneous quench* for both initial conditions such that their chemical potentials are quenched to μ and T_i is quenched to T. The parameters after quench can be higher or lower than their values before quench. We follow the time evolution of an entity for I and II to see if they cross each other at some finite time $\tau > 0$ before reaching the same steady state, and thereby if that entity exhibits QMPE. We investigate QMPE in the density matrix elements, and in the temperature to explicitly survey the possibility of thermal QMPE.

QMPE in density matrix elements.—The time evolution of $\rho_\alpha(\tau)$ ($\alpha = 1, 2, 3, 4$) is governed by the eigenvalues and (right and left) eigenvectors of $\hat{K}$ [Eq. (3)]. The formal expressions of $\rho_\alpha(\tau)$, for I and II, are

$$\rho_\alpha^{\mathrm{I}}(\tau) = \sum_{n=1}^{4} e^{\lambda_n \tau} \hat{R}_{\alpha,n} a_n^{\mathrm{I}}, \qquad a_n^{\mathrm{I}} = \sum_{m=1}^{4} \hat{L}_{n,m} \rho_m^{\mathrm{I}}(0),$$
$$\rho_\alpha^{\mathrm{II}}(\tau) = \sum_{n=1}^{4} e^{\lambda_n \tau} \hat{R}_{\alpha,n} a_n^{\mathrm{II}}, \qquad a_n^{\mathrm{II}} = \sum_{m=1}^{4} \hat{L}_{n,m} \rho_m^{\mathrm{II}}(0), \tag{5}$$

where λ_n ($n = 1, 2, 3, 4$) are the eigenvalues of $\hat{K}$ such that $\lambda_1 > \lambda_2 > \lambda_3 > \lambda_4$. Here λ_1 ($= 0$) and λ_2 correspond to the steady state and the slowest relaxation mode, respectively. The matrices $\hat{R}$ and $\hat{L}$ consist of the right eigenvectors and left eigenvectors of $\hat{K}$, respectively [58]. The coefficients $a_n^{\mathrm{I,II}}$ [Eq. (5)] contain the effects of the initial conditions. In many literature, only the coefficients $a_2^{\mathrm{I,II}}$, corresponding to the slowest eigenmode, is considered to analyze the MPE at sufficiently large time where the effects of other coefficients $a_n^{\mathrm{I,II}}$ ($n > 2$) are assumed negligible [30,40,45,48]. Several studies concentrate on engineering special initial conditions that lead to $a_2 = 0$ [45,49] causing strong MPE with exponentially faster relaxation. In this connection, we have found an intriguing fact that the Anderson model of QD satisfies the condition

$$a_2^{\mathrm{I}} = a_2^{\mathrm{II}} = 0, \tag{6}$$

irrespective of the particulars of initial conditions and parameter values. The slowest relaxation mode λ_2 does not contribute to the time evolved density matrix elements and other observables, for any initial condition distributed in the steady state form. Thus, the coefficients $a_2^{\mathrm{I,II}}$ are not appropriate to discuss QMPE for the Anderson model.

This naturally raises the following question: what are the roles of the coefficients a_3 and a_4, corresponding to the remaining relaxation modes $n = 3, 4$, in producing QMPE? To answer this, we consider the difference between the time evolutions of density matrix elements starting from I and II; i.e.,

$$\Delta\rho_\alpha(\tau) \coloneqq \rho_\alpha^{\mathrm{I}}(\tau) - \rho_\alpha^{\mathrm{II}}(\tau), \qquad \alpha = 1, 2, 3, 4. \tag{7}$$

To obtain QMPE, we have to make sure that some $\Delta\rho_\alpha(\tau_\alpha) = 0$ at finite time $\tau = \tau_\alpha$. We obtain the following analytical expressions for $\Delta\rho_\alpha(\tau)$:

$$\Delta\rho_\alpha(\tau) = e^{\lambda_3\tau}\hat{R}_{\alpha,4}\Delta a_4[S_\alpha + e^{-(\lambda_3-\lambda_4)\tau}], \tag{8}$$

where $S_\alpha \coloneqq (\hat{R}_{\alpha,3}\Delta a_3)/(\hat{R}_{\alpha,4}\Delta a_4)$ and $\Delta a_\alpha \coloneqq a_\alpha^{\mathrm{I}} - a_\alpha^{\mathrm{II}}$. Since the expression of S_α explicitly depends on the ratio $\Delta a_3/\Delta a_4$, we conclude that QMPE in the density matrix elements is dictated by *both* the surviving relaxation modes rather than only one of them. Since in Eq. (8), $0 \leq e^{-(\lambda_3-\lambda_4)\tau} \leq 1$, the *necessary* condition to ensure QMPE in $\rho_\alpha(\tau)$ is

$$S_\alpha < 0 \quad \text{and} \quad |S_\alpha| < 1. \tag{9}$$

Note that we have not used the explicit expressions of the eigenvalues and eigenvectors of $\hat{K}$ to derive the criterion Eq. (9). One can control one or more parameters from $(\mu_L^{\mathrm{I}}, \mu_R^{\mathrm{I}}, \mu^{\mathrm{II}}, T_i; \mu, T)$. We choose to vary μ_L^{I} or μ_R^{I} or both. We denote the number of density matrix elements showing QMPE by $\nu(\hat{\rho})$, which can take one of the four possible values 0, 1, 2, or 3.

In Fig. 1, we present the variation of $\nu(\hat{\rho})$ in the $\beta\mu_L^{\mathrm{I}} - \beta\mu_R^{\mathrm{I}}$ plane, where $\beta = 1/T$. This figure is constructed by directly implementing the criterion in Eq. (9). The parameter plane captures all possible values of $\nu(\hat{\rho})$. The behavior of $\nu(\hat{\rho})$ is naturally symmetric with respect to $\beta\mu_L^{\mathrm{I}}$ and $\beta\mu_R^{\mathrm{I}}$. A quadrant centering $\beta\mu_L^{\mathrm{I}} = \beta\mu_R^{\mathrm{I}} = 0$ appears on the plane that forbids the occurrence of QMPE and is characterized by $\nu(\hat{\rho}) = 0$. As we move away from this quadrant, the density matrix elements start showing QMPE. If we fix one of the parameters $\beta\mu_L^{\mathrm{I}}$ and $\beta\mu_R^{\mathrm{I}}$ and increase the other, the value of $\nu(\hat{\rho})$ does not increase monotonically in the order of $\nu(\hat{\rho}) = 0$, 1, 2, 3; rather we have a narrow parameter region exhibiting $\nu(\hat{\rho}) = 3$ sandwiched between regions showing $\nu(\hat{\rho}) = 1$ and $\nu(\hat{\rho}) = 2$. The fact that the parameter regions showing $\nu(\hat{\rho}) = 3$ or 1 are much narrower than the regions displaying $\nu(\hat{\rho}) = 2$ or 0 is generic for our model [58].

Since QMPE is a dynamical phenomenon, we characterize the occurrence of QMPE in $\hat{\rho}$ by the *temporal* order parameter defined as

$$\begin{aligned} &\tilde{\tau}(\hat{\rho}) = \max[\tau_1, \tau_2, \tau_3, \tau_4] \quad \text{if } 0 < \tau_\alpha < \infty, \\ &\tilde{\tau}(\hat{\rho}) \to \infty \quad \text{if no finite } \tau_\alpha \text{ exists} \quad \forall\, \alpha, \end{aligned} \tag{10}$$

where τ_α ($\alpha = 1$, 2, 3, 4) is the solution of $\Delta\rho_\alpha(\tau_\alpha) = 0$, and $\max[x_1, x_2, x_3, x_4]$ selects the largest x_i among x_1, x_2, x_3, and x_4. The reason to focus on the maximum among τ_αs in Eq. (10) is to detect the largest time which bears the memory effect from the initial quench. The trivial steady state solution $\Delta\rho_\alpha(\tau \to \infty) = 0\ \forall\ \alpha$ must be avoided. In Fig. 2, we present the behavior of $\tilde{\tau}(\hat{\rho})$ in the $\beta\mu_L^{\mathrm{I}} - \beta\mu_R^{\mathrm{I}}$ plane. The majority of the parameter region exhibits QMPE with largest $\tilde{\tau}(\hat{\rho})$ of the order of unity. The proposed order parameter provides prominent boundaries demarcating regions with and without QMPE. To reduce the number

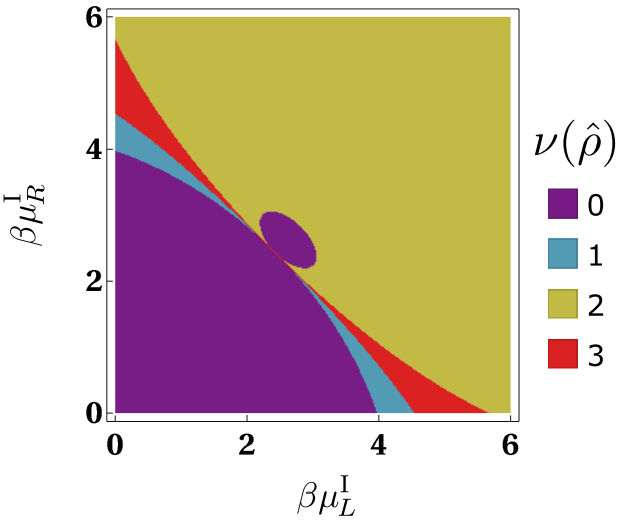

FIG. 1. Illustration of different regions in the $\beta\mu_L^{\mathrm{I}} - \beta\mu_R^{\mathrm{I}}$ plane with distinct values of $\nu(\hat{\rho})$ (number of density matrix elements showing QMPE). Parameters used are $\beta\epsilon_0 = 2.0$, $\beta U = 1.25$, $\beta\mu^{\mathrm{II}} = 2.43$, $\beta T_i = 1.15$, $\beta\mu = 2.0$.

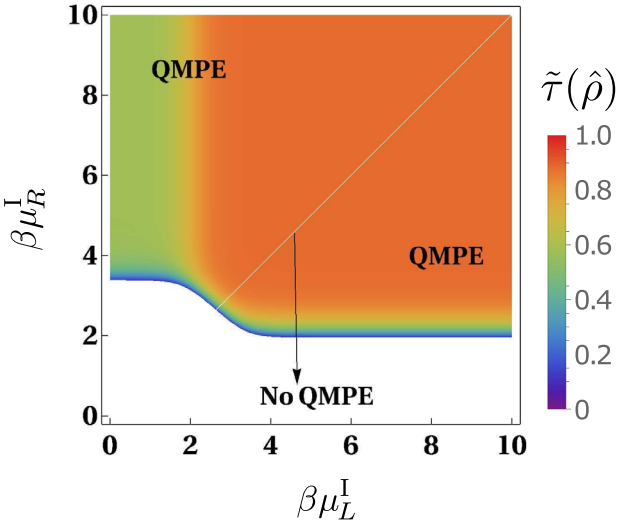

FIG. 2. QMPE for $\hat{\rho}$ in $\beta\mu_L^{\mathrm{I}} - \beta\mu_R^{\mathrm{I}}$ plane characterized by $\tilde{\tau}(\hat{\rho})$ [Eq. (10)]. The white regions represent the absence of QMPE. Parameters used are $\beta\epsilon_0 = 2.0$, $\beta U = 1.25$, $\beta T_i = 0.25$, $\beta\mu = 2.0$, and $\beta\mu^{\mathrm{II}} = \beta\mu_R^{\mathrm{I}}$.

of independent parameters we consider $\beta\mu^{\mathrm{II}} = \beta\mu_R^{\mathrm{I}}$ in Fig. 2. However, such a special scenario creates asymmetric nature of $\tilde{\tau}(\hat{\rho})$ with respect to $\beta\mu_L^{\mathrm{I}}$ and $\beta\mu_R^{\mathrm{I}}$, evident in Fig. 2. Notably, for fixed $\beta\mu_R^{\mathrm{I}} < 2$, QMPE is prohibited in the whole tunable range of $\beta\mu_L^{\mathrm{I}}$ (0 to ∞).

QMPE in system temperature.—Next we investigate the possibility of QMPE in the system temperature, i.e., quantum counterpart of the original MPE. The concept of temperature has to be *dynamical* as we study the temporal relaxation of the system. The process of thermalization itself can be tricky for quantum systems [59–61]. Nevertheless, we use the definition of time dependent temperature $T_s(\tau)$ [62] as

$$T_s(\tau) := \frac{\partial E_s(\tau)}{\partial S_{\mathrm{vN}}(\tau)} = \frac{\partial E_s(\tau)}{\partial \tau} \Big/ \frac{\partial S_{\mathrm{vN}}(\tau)}{\partial \tau}, \tag{11}$$

where $S_{\mathrm{vN}}(\tau) = -\sum_\alpha \rho_\alpha(\tau) \ln[\rho_\alpha(\tau)]$ is the von Neumann entropy and $E_s(\tau) = \mathrm{Tr}[\hat{\rho}(\tau)\hat{H}_s]$ is the average energy. The thermalization and the validity of the system temperature are ensured from the checked fact that different initial conditions converge to the identical steady state value $T_s(\tau \to \infty)$. Also, the classical limit is recovered as $T_s(\tau \to \infty)$ matches with the reservoir temperature T when the Fermi-Dirac distribution [Eq. (4)] can be approximated as Maxwell-Boltzmann distribution [58].

Interestingly, in Fig. 3, we observe that $\beta T_s(\tau)$ starting from two different initial values cross each other at a finite time showing QMPE. Since both the initial temperatures are higher than the steady state value, this QMPE involves cooling processes where the initially hotter system becomes colder after the crossing, and thereby produces the *normal* QMPE [28]. It is fascinating that the QD indeed generates thermal MPE. The inset of Fig. 3 confirms that both initial temperatures reach the same steady state.

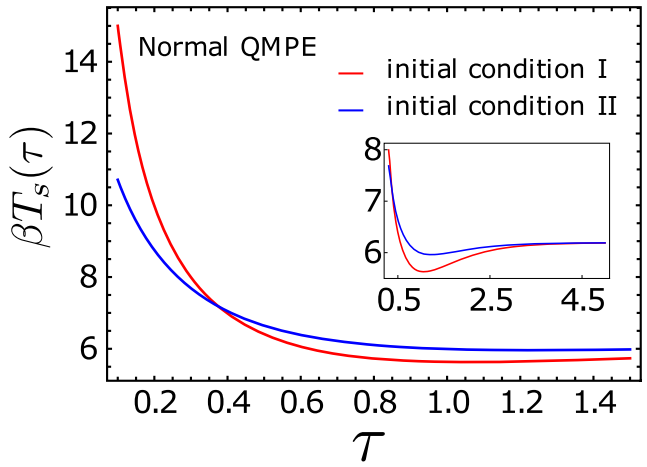

FIG. 3. Thermal QMPE where temperatures [Eq. (11)] starting from two different initial conditions cross each other at finite time. The inset shows their convergence to the same steady state. Parameters used are $\beta\epsilon_0 = 2.0$, $\beta U = 1.25$, $\beta\mu_L^{\mathrm{I}} = 4.5$, $\beta\mu_R^{\mathrm{I}} = 1.0$, $\beta\mu^{\mathrm{II}} = 2.43$, $\beta T_i = 1.15$, $\beta\mu = 2.0$.

We should examine if the occurrence of thermal QMPE in Fig. 3 is an isolated incident in a rather large parameter space. For this purpose, analogous to $\tilde{\tau}(\hat{\rho})$ [Eq. (10)], we define $\tilde{\tau}(T_s)$ characterizing thermal QMPE as

$$\begin{aligned} 0 < \tilde{\tau}(T_s) < \infty &: \text{thermal QMPE}, \\ \tilde{\tau}(T_s) \to \infty &: \text{no QMPE}, \end{aligned} \tag{12}$$

where $\tilde{\tau}(T_s)$ is the solution of $\Delta T_s(\tilde{\tau}) = 0$, with $\Delta T_s := T_s^{\mathrm{I}} - T_s^{\mathrm{II}}$. In Fig. 4, we present the behavior of $\tilde{\tau}(T_s)$ with the variation of $\beta\mu_L^{\mathrm{I}}$. This remarkably rich diagram reveals that thermal QMPE is rather generic than occasional. We observe large parameter ranges exhibiting normal QMPE (an example being Fig. 3) and *mixed* QMPE (one of the initial temperatures is lower than the steady state value) [28], with the intermediate region displaying the absence of QMPE. The model is also capable to exhibit *inverse* QMPE [58] (both initial temperatures are lower than the steady state value [19]), although the inverse QMPE is much weaker than normal and mixed QMPEs. An interesting observation is that most of the parameter regions demonstrating normal QMPE are associated with nonanalyticity in the system temperature (Fig. 4, inset) resulting in dynamical quantum phase transition (QPT) [63]. The negative temperature (Fig. 4, inset) originates from the *nonmonotonicity* of the entropy while the energy changes monotonically. Negative temperatures along with bounded energy spectrum have been predicted [64,65] and experimentally observed [66,67] for two-dimensional vortices, localized spin systems [68–70], bosonic single mode cavity [62], etc. The thermal QMPE in the present model remains

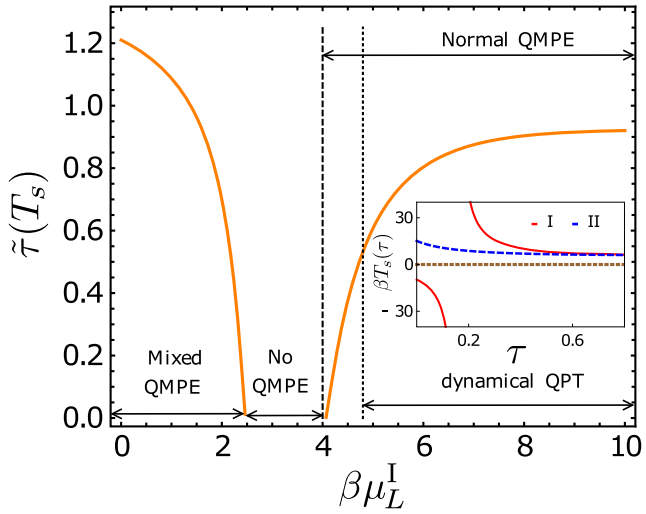

FIG. 4. Variation of $\tilde{\tau}(T_s)$ [Eq. (12)] characterizing thermal QMPE. We observe mixed QMPE and normal QMPE, separated by a region with no thermal QMPE. A majority of the parameter range showing normal QMPE is associated with dynamical QPT (inset). Parameters used are $\beta\epsilon_0 = 2.0$, $\beta U = 1.25$, $\beta\mu_R^{\mathrm{I}} = 1.0$, $\beta\mu^{\mathrm{II}} = 2.43$, $\beta T_i = 1.15$, $\beta\mu = 2.0$.

unaffected by the dynamical QPT as $\tilde{\tau}(T_s)$ increases continuously across the borderline demarcating the presence and absence of dynamical QPT.

Apart from temperature and density matrix, energy, von Neumann entropy and Kullback-Leibler divergence $[D_{\mathrm{KL}}(\tau)]$ can also exhibit QMPE [58]. Remarkably, we have found parameter regions where thermal QMPE is observed but $D_{\mathrm{KL}}(\tau)$ does not show QMPE and vice versa, implying that here $D_{\mathrm{KL}}(\tau)$ cannot act as an alternative indicator for thermal QMPE [58]. We observe that higher initial difference between initial and steady state goes faster to zero for QMPE in energy and entropy [58]. Similar observation regarding faster restoration of more initially broken symmetry has been studied recently using entanglement asymmetry [47].

Summary.—We have demonstrated QMPE in a single-level quantum dot coupled to two reservoirs, described by the Anderson model. Interestingly, the slowest relaxation mode which has been by far the only focus for producing MPE in Markovian systems has no contribution to QMPE for the Anderson model. Rather, we have presented the necessary criterion, involving the combination of remaining relaxation modes, to obtain QMPE in the density matrix elements. We have achieved the thermal QMPE in the temperature where an initially hotter system can cool faster than an initially colder system and they reverse their identities (hotter becomes colder and vice versa) after some finite time.

It would be important to investigate the thermal QMPE in other quantum systems and systematically establish the general framework for it. We wish to explore the connection of symmetry breaking to QMPE [47] in quantum dots. There have been several experiments on QD [71–77], including single-level QD coupled to two leads with different chemical potentials and controlled by gate voltages [76,77]. Thus, it is straightforward to perform experiments on QMPE by controlling chemical potentials discussed in this Letter.

We thank Frédéric van Wijland, Raphael Chetrite, Marija Vucelja, Ryo Hanai, Manas Kulkarni, Amit Dey, and Brett Min for useful discussions. This work is partially supported by the Grants-in-Aid for Scientific Research (Grants No. 21H01006 and No. 20K14428). A. K. C. gratefully acknowledges support from a postdoctoral fellowship from the YITP. The numerical calculations have been done on Yukawa-21 at the YITP.

*ak.chatterjee@yukawa.kyoto-u.ac.jp
†takada@go.tuat.ac.jp
‡hisao@yukawa.kyoto-u.ac.jp

[1] *Aristotle's Metaphysics*, translated by W. D. Ross (Clarendon, Oxford, 1981).
[2] E. B. Mpemba and D. G. Osborne, Phys. Educ. **4**, 172 (1969).
[3] M. Vynnycky and N. Maeno, Int. J. Heat Mass Transfer **55**, 7297 (2012).
[4] M. Vynnycky and S. Kimura, Int. J. Heat Mass Transfer **80**, 243 (2015).
[5] S. M. Mirabedin and F. Farhadi, Int. J. Refrig. **73**, 219 (2017).
[6] M. Vynnycky and S. Mitchell, Heat Mass Transfer **46**, 881 (2010).
[7] D. Auerbach, Am. J. Phys. **63**, 882 (1995).
[8] B. Wojciechowski, I. Owczarek, and G. Bednarz, Cryst. Res. Technol. **23**, 843 (1988).
[9] X. Zhang, Y. Huang, Z. Ma, Y. Zhou, J. Zhou, W. Zheng, Q. Jiang, and C. Q. Sun, Phys. Chem. Chem. Phys. **16**, 22995 (2014).
[10] J. I. Katz, Am. J. Phys. **77**, 27 (2009).
[11] J. D. Brownridge, Am. J. Phys. **79**, 78 (2011).
[12] A. Gijón, A. Lasanta, and E. R. Hernández, Phys. Rev. E **100**, 032103 (2019).
[13] H. C. Burridge and P. F. Linden, Sci. Rep. **6**, 37665 (2016).
[14] P. Chaddah, S. Dash, K. Kumar, and A. Banerjee, arXiv:1011.3598.
[15] Y.-H. Ahn, H. Kang, D.-Y. Koh, and H. Lee, Korean J. Chem. Eng. **33**, 1903 (2016).
[16] C. Hu, J. Li, S. Huang, H. Li, C. Luo, J. Chen, S. Jiang, and L. An, Cryst. Growth Des. **18**, 5757 (2018).
[17] A. Kumar and J. Bechhoefer, Nature (London) **584**, 64 (2020).
[18] A. Kumar, R. Cheétrite, and J. Bechhoefer, Proc. Natl. Acad. Sci. U.S.A. **119**, e2118484119 (2022).
[19] A. Lasanta, F. Vega Reyes, A. Prados, and A. Santos, Phys. Rev. Lett. **119**, 148001 (2017).
[20] A. Torrente, M. A. López-Castaño, A. Lasanta, F. V. Reyes, A. Prados, and A. Santos, Phys. Rev. E **99**, 060901(R) (2019).
[21] A. Biswas, V. V. Prasad, O. Raz, and R. Rajesh, Phys. Rev. E **102**, 012906 (2020).
[22] A. Biswas, V. V. Prasad, and R. Rajesh, Europhys. Lett. **136**, 46001 (2021).
[23] E. Mompó, M. A. López Castaño, A. Torrente, F. Vega Reyes, and A. Lasanta, Phys. Fluids **33**, 062005 (2021).
[24] A. Megias and A. Santos, Front. Phys. **10**, 971671 (2022).
[25] T. Keller, V. Torggler, S. B. Jäger, S. Schütz, H. Ritsch, and G. Morigi, New J. Phys. **20**, 025004 (2018).
[26] A. Santos and A. Prados, Phys. Fluids **32**, 072010 (2020).
[27] A. Patrón, B. Sánches-Rey, and A. Pradros, Phys. Rev. E **104**, 064127 (2021).
[28] S. Takada, H. Hayakawa, and A. Santos, Phys. Rev. E **103**, 032901 (2021).
[29] S. Takada, Eur. Phys. J. Web Conf. **249**, 04001 (2021).
[30] Z. Lu and O. Raz, Proc. Natl. Acad. Sci. U.S.A. **114**, 5083 (2017).
[31] I. Klich, O. Raz, O. Hirschberg, and M. Vucelja, Phys. Rev. X **9**, 021060 (2019).
[32] D. M. Busiello, D. Gupta, and A. Maritan, New J. Phys. **23**, 103012 (2021).
[33] J. Lin, K. Li, J. He, J. Ren, and J. Wang, Phys. Rev. E **105**, 014104 (2022).
[34] P. A. Greaney, G. Lani, G. Cicero, and J. C. Grossman, Metall. Mater. Trans. A **42**, 3907 (2011).

[35] M. Baity-Jesi *et al.*, Proc. Natl. Acad. Sci. U.S.A. **116**, 15350 (2019).
[36] R. G. González, N. Khalil, and V. Garzó, Phys. Fluids **33**, 053301 (2021).
[37] Z.-Y. Yang and J.-X. Hou, Phys. Rev. E **101**, 052106 (2020).
[38] Z.-Y. Yang and J.-X. Hou, Phys. Rev. E **105**, 014119 (2022).
[39] I. González-Adalid Pemartín, E. Mompó, A. Lasanta, V. Martín-Mayor, and J. Salas, Phys. Rev. E **104**, 044114 (2021).
[40] R. Cheétrite, A. Kumar, and J. Bechhoefer, Front. Phys. **9**, 654271 (2021).
[41] R. Holtzman and O. Raz, Commun. Phys. **5**, 280 (2022).
[42] A. Megias, A. Santos, and A. Prados, Phys. Rev. E **105**, 054140 (2022).
[43] A. Biswas, V. V. Prasad, and R. Rajesh, arXiv:2303.10900.
[44] A. Nava and M. Fabrizio, Phys. Rev. B **100**, 125102 (2019).
[45] F. Carollo, A. Lasanta, and I. Lesanovsky, Phys. Rev. Lett. **127**, 060401 (2021).
[46] S. K. Manikandan, Phys. Rev. Res. **3**, 043108 (2021).
[47] F. Ares, S. Murciano, and P. Calabrese, Nat. Commun. **14**, 2036 (2023).
[48] F. Ivander, N. Anto-Sztrikacs, and D. Segal, arXiv:2301.06135.
[49] M. R. Walker and M. Vucelja, J. Stat. Mech. (2021) 113105.
[50] R. Yoshii and H. Hayakawa, arXiv:1312.3772.
[51] H. Hayakawa, V. M. M. Paasonen, and R. Yoshii, arXiv:2112.12370.
[52] R. Yoshii and H. Hayakawa, Phys. Rev. Res. **5**, 033014 (2023).
[53] S. Nakajima, M. Taguchi, T. Kubo, and Y. Tokura, Phys. Rev. B **92**, 195420 (2015).
[54] S. M. Cronenwett, T. H. Oosterkamp, and L. P. Kouwenhoven, Science **281**, 540 (1998).
[55] R. Sakano and N. Kawakami, Phys. Rev. B **73**, 155332 (2006).
[56] R. Hiraoka, E. Minamitani, R. Arafune, N. Tsukahara, S. Watanabe, M. Kawai, and N. Takagi, Nat. Commun. **8**, 16012 (2017).
[57] A. J. Keller, J. S. Lim, D. Sánchez, R. López, S. Amasha, J. A. Katine, H. Shtrikman, and D. Goldhaber-Gordon, Phys. Rev. Lett. **117**, 066602 (2016).
[58] See Supplemental Material at http://link.aps.org/supplemental/10.1103/PhysRevLett.131.080402 for eigenvalues and eigenvectors of transition matrix, mixed QMPE, inverse QMPE and QMPE in energy, von-Neumann entropy and Kullback-Leibler divergence.
[59] R. Nandkishore and D. A. Huse, Annu. Rev. Condens. Matter Phys. **6**, 15 (2015).
[60] T. Mori, T. N. Ikeda, E. Kaminishi, and M. Ueda, J. Phys. B **51**, 112001 (2018).
[61] N. Shiraishi and K. Matsumoto, Nat. Commun. **12**, 5084 (2021).
[62] M. M. Ali, W-M. Huang, and W-M. Zhang, Sci. Rep. **10**, 13500 (2020).
[63] M. Heyl, Rep. Prog. Phys. **81**, 054001 (2018).
[64] L. Onsager, Nuovo Cimento **6**, 279 (1949).
[65] L. D. Landau and E. M. Lifshitz, *Statistical Physics. Part 1* (Pergamon Press, Oxford, 1980), p. 449.
[66] G. Gauthier, M. T. Reeves, X. Yu, A. S. Bradley, M. A. Baker, T. A. Bell, H. Rubinsztein-Dunlop, M. J. Davis, and T. W. Neely, Science **364**, 1264 (2019).
[67] S. P. Johnstone, A. J. Groszek, P. T. Starkey, C. J. Billinton, T. P. Simula, and K. Helmerson, Science **365**, 1267 (2019).
[68] N. F. Ramsey, Phys. Rev. **103**, 20 (1956).
[69] E. M. Purcell and R. V. A. Pound, Phys. Rev. **81**, 279 (1951).
[70] P. Medley, D. M. Weld, H. Miyake, D. E. Pritchard, and W. Ketterle, Phys. Rev. Lett. **106**, 195301 (2011).
[71] L. D. Winkler, J. F. Arceo, W. C. Huges, B. A. DeGraff, and B. H. Augustine, J. Chem. Educ. **82**, 1700 (2005).
[72] G. Fève, A. Mahé, J.-M. Berroir, T. Kontos, B. Placais, D. C. Glattli, A. Cavanna, B. Etienne, and Y. Jin, Science **316**, 1169 (2007).
[73] M. D. BLumenthal, B. Kaestner, L. Li, S. Giblin, T. J. B. M. Janssen, M. Pepper, D. Anderson, G. Jones, and D. A. Ritchie, Nat. Phys. **3**, 343 (2007).
[74] M. R. Connolly, K. L. Chiu, S. P. Giblin, M. Kataoka, J. D. Fletcher, C. Chua, J. P. Griffiths, G. A. C. Jones, V. I. Falko, C. G. Smith, and T. J. B. M. Janssen, Nat. Nanotechnol. **8**, 417 (2013).
[75] M. Liu, N. Yazdani, M. Yarema, M. Jansen, V. Wood, and E H. Sargent, Nat. Electron. **4**, 548 (2021).
[76] D. M. T. van Zanten, D. M. Basko, I. M. Khaymovich, J. P. Pekola, H. Courtois, and C. B. Winkelmann, Phys. Rev. Lett. **116**, 166801 (2016).
[77] A. García Corral, D. M. T. van Zanten, K. J. Franke, H. Courtois, S. Florens, and C. B. Winkelmann, Phys. Rev. Res. **2**, 012065(R) (2020).